Multiscale analysis of heat transfer in fully developed turbulent channel flow

T. Wei
Department of Mechanical Engineering, University of Utah, Salt Lake City, UT 84112

P. Fife
Department of Mathematics University of Utah

J. Klewicki, P. McMurtry
Department of Mechanical Engineering, University of Utah

July 7, 2005

Abstract

An analysis is given for fully developed thermal transport through a wall-bounded turbulent fluid with constant heat flux supplied at the boundary. The analysis proceeds from the averaged heat equation and utilizes, as principal tools, various scaling considerations. The paper first provides an accounting of the relative dominance of the three terms in that averaged equation, based on existing DNS data. The results show a clear decomposition of the turbulent layer into zones, each with its characteristic transport mechanisms. There follows a theoretical treatment which justifies and greatly extends these empirical results. The main hypothesis in this development is the monotone and limiting dependence of the difference between the specially scaled centerline and wall temperatures on the Prandtl number, a fact well corroborated by DNS data. A fairly complete qualitative and order-of-magnitude quantitative picture emerges for a complete range in Prandtl numbers. It agrees with known empirical information. In a manner similar to previous analyses of turbulent fluid flow in a channel, conditions for the existence or nonexistence of logarithmic-like profiles are found.

1 Introduction

Convective heat transfer from surfaces beneath wall bounded flows impact a large number of technologically important applications [1, 2]. Of course, if the flow is turbulent, the rate of this heat transfer is significantly augmented relative to the laminar flow condition [2]. A substantial body of evidence [3] points to important connections between the mechanisms for this enhanced rate of heat transfer and those affecting momentum transport that, for example, also underlie the enhanced surface shear stress in such flows. These connections between momentum and heat transport provide a level of justification for the popular analogy-based correlations often employed in practical engineering computation strategies, e.g., [1, 2]. At perhaps an even more pervasive level, these connections also often constitute part or all of the conceptual framework for describing the physics of turbulent heat transfer. Somewhat contrary to such notions, however, is the considerable body of evidence indicating that turbulent scalar fields can exhibit behaviors distinct and neither intuitively connected nor rationally predictable from an understanding of the momentum field alone [4]. Divergent behaviors between the statistical properties of the momentum and scalar fields become

especially apparent in non-canonical flows, where effects such as surface curvature and pressure gradients are present, e.g., [5]. Relative to general heat transfer prediction, these observations would seem to indicate that momentum and scalar transport are more tenuously (or at least more subtly) related than the popular analogies might lead one to believe. Such considerations motivate the present objectives to more clearly elucidate the relative importance of the underlying mechanisms for turbulent heat transfer near walls, their scaling behaviors and their connections to the fluid dynamical mechanisms.

The most common point of departure for addressing the problem of turbulent heat transfer near walls involves simultaneous consideration of the appropriately simplified, once-integrated, time averaged, differential equations describing the conservation of linear momentum and thermal energy, e.g., [2, 6]. Of course, the process of time averaging yields the classical closure problem(s) in which the momentum and energy equations are indeterminate owing to the presence of the kinematic Reynolds shear stress, $\langle uv \rangle$, and turbulent heat flux, $\langle v\theta \rangle$, respectively. Attempts to close these equations have invoked various phenomenological models [3, 7, 8]. Prevalent among such models are those that employ the eddy viscosity, ν_t, and mixing length, ℓ_m, concepts, and by analogy the notion of a turbulent Prandtl number, Pr_t. Regarding the efficacy of such approaches, the recent efforts of Churchill and his co-workers [9, 10, 11] are particularly noteworthy. In these studies they invoke a novel local normalization of the Reynolds shear stress and turbulent heat flux. Significantly, consideration of the aforementioned, once-integrated, forms of momentum and energy equations reveals rigorously defined functions for the eddy viscosity, mixing length and turbulent Prandtl number in terms of these locally normalized functions. Relative to the development of improved conceptual understanding, an important outcome of this analysis is that ν_t, ℓ_m and Pr_t are shown to be derivable independently of their phenomenological origins (associated with "turbulent diffusion"), and in fact are perhaps best interpreted simply as those functions required to close their respective indeterminate equations. Furthermore, Churchill et al. show that normalization of the local turbulent heat flux by the total local heat flux (or similarly, the Reynolds stress by the total shear stress) leads to an attractive framework for constructing accurate correlating equations (i.e., curve fits) having considerable applied utility.

Owing to their implicit, and sometimes explicit, empiricism, however, these and other similar methodologies do not optimally serve the present objectives, since, for example, the connections between the functional form of any given correlating equation and the true scaling behaviors describing the underlying transport mechanisms are not rigorously established. Perhaps even more significantly, these (and most other approaches) begin with the once-integrated form of the equations. In this regard it is crucial to note that the once-integrated form of, for example, the force balance no more reflects the basic properties and scaling behaviors of the mean dynamics than the twice-integrated form; otherwise known as the equation for the undifferentiated mean velocity function. Through an analysis of the actual mean momentum balance (the terms of which comprise stress gradients rather than stresses), Wei et al [12] have revealed an alternative physical/theoretical framework for describing flow structure. This framework includes a structure for wall-bounded turbulent flows that differs considerably from the nearly universally accepted sub-, buffer, logarithmic and wake, layer structure. In doing so, it also, for example, unambiguously reveals that viscous forces affect dynamics much farther into the flow from the wall than previously believed. Furthermore, this framework has provided the impetus for follow-on studies [13, 14, 15, 16] that respectively, *i*) reveal the existence of a mathematical scaling hierarchy throughout a significant portion of the flow whose properties, for example, rigorously establish necessary conditions for a logarithmic mean velocity profile, *ii*) enable the development of a physical model that, for the

first time, explicitly embodies a consistent dynamical relationship with the properties of the mean momentum balance, and *iii*) establish new scaling laws for the Reynolds stress that are derived directly through the manipulation of the equation for mean flow dynamics. More broadly, these efforts clarify that the physical/mathematical interpretations of the unintegrated form of the mean momentum balance are uniquely associated with the mechanisms describing the time rate of change of mean momentum, while the first integral of this equation has a distinctly different interpretation; describing the mechanisms associated with the contributions to the flux of momentum.

The present study initiates exploration of the fundamental behaviors of turbulent heat transfer in wall-bounded flows by following the same strategy employed by Wei et al [12] and subsequent papers in their study of mean flow dynamics. Specifically, the scope of the present effort involves use of available high resolution data to examine the behavior by which the unintegrated form of the mean energy equation is balanced. From this the layer structure of the thermal energy field and its scaling behaviors (relative to variations in Reynolds number and Prandtl number) are revealed.

As mentioned above, past theoretical approaches to turbulent heat transfer have largely been based on hypotheses designed to close the Reynolds averaged equation for the mean velocity and mean temperature, or on dimensional considerations. The closure hypotheses usually involve quantities that are rarely measured directly, or that are impossible to measure accurately with current techniques. As stated by Perry and Schofield, "*The physical basis of the closing hypotheses is of limited soundness, and the ultimate success of this approach seems doubtful.*" [17].

Therefore it seems reasonable to try another approach and to ascertain the scaling behaviors of turbulent heat transfer as revealed by an analysis of the equations alone. Of course, it should not be expected that these arguments alone will yield a complete solution of the problem. However, recent studies [12, 13, 14, 15, 16] of the averaged momentum equation in analogous contexts show that scaling properties and much flow physics can be found through such methodologies.

Sec. 2 is devoted to deriving and explaining the basic averaged heat equation and boundary conditions that will be used in the paper. Especially noteworthy is the non-traditional temperature unit (9) found to be appropriate. The flow is shown in Sec. 3 to be partitioned into four zones according to the relative dominance of the three heat transport terms in the basic energy balance equation derived in Sec. 2. An extensive multiscale analysis of the basic scaled heat equation is begun in Sec. 4. This analysis is shown to depend strongly on the Prandtl number Pr. When $Pr \ll 1$, there is only one appropriate scaling of the variables. In particular, distance from the wall is scaled by the usual outer scaling, even near the wall, and temperature is measured by the new unit mentioned before. When $Pr \gg 1$, however, the magnitude of the centerline scaled temperature serves as proper small parameter with which to build asymptotics for inner, outer, and mesolayers. That magnitude depends monotonically on Pr. Previous analysis of the flow structure of turbulent channel flow provides a paradigm for this construction. Finally Sec. 5 is devoted to extending that paradigm to account for a continuum of scaling patches, in addition to the three already studied, which altogether cover a good part of the channel cross section. It is in Sec. 5 that the relevance of this continuum to the question of the logarithmic nature of the mean temperature profile is brought to light.

UU IR Author Manuscript

2 Derivation of the model

2.1 The heat equation

A detailed derivation of the heat transfer equation for turbulent wall bounded flows appears, for example, in the books by Monin and Yaglom [6] , Landau and Lifshitz [18] and Kays and Crawford [2]. Since the present paper relies heavily on the analysis of the mean heat equation, it is appropriate to repeat the derivation briefly. For incompressible flow with constant properties and with viscous dissipation neglected, the instantaneous energy equation is given by

$$\frac{\partial\tilde{\theta}}{\partial\tau}+\tilde{u}_j\frac{\partial\tilde{\theta}}{\partial x_j}=\alpha\frac{\partial^2\tilde{\theta}}{\partial x_j\partial x_j}, \tag{1}$$

where $\tilde{\theta}$ and $\tilde{u}_j$ are the instantaneous temperature and velocity, τ is time, and α is the molecular thermal diffusivity. The dimension of α is the same as that of the kinematic molecular viscosity ν, $\left[\frac{L^2}{\tau}\right]$. The Prandtl number is defined by the ratio, $Pr=\frac{\nu}{\alpha}$. The heat equation is very similar in form to that of the momentum equation, except there is no pressure term in the former.

The averaged heat equation is

$$\frac{\partial\Theta}{\partial\tau}+U_j\frac{\partial\Theta}{\partial x_j}=\frac{\nu}{Pr}\frac{\partial^2\Theta}{\partial x_j\partial x_j}-\frac{\partial\langle u_j\theta\rangle}{\partial x_j} \tag{2}$$

where the decomposition of $\tilde{\theta}$ and $\tilde{u}$ into their mean and fluctuating parts is given by

$$\tilde{\theta}=\Theta+\theta;\quad \tilde{u}_j=U_j+u_j, \tag{3}$$

and averaging is denoted by $\langle\cdot\rangle$. For the details of the averaging procedure one is referred, e.g., to Monin and Yaglom [6].

For stationary 2-D boundary layers, the standard boundary layer simplification reduces the heat equation to

$$U\frac{\partial\Theta}{\partial x}+V\frac{\partial\Theta}{\partial y}=\frac{\nu}{Pr}\frac{\partial^2\Theta}{\partial y^2}-\frac{\partial\langle v\theta\rangle}{\partial y}, \tag{4}$$

where $(U,V)=(U_1,U_2)$, etc.

In the case of steady channel flow, there is no mean motion normal to the wall and the heat equation is further simplifed to

$$U\frac{\partial\Theta}{\partial x}=\frac{\nu}{Pr}\frac{\partial^2\Theta}{\partial y^2}-\frac{\partial\langle v\theta\rangle}{\partial y} \tag{5}$$

Traditionally the friction temperature (Kader et al. [3] calls it the heat flux temperature) is defined by

$$\theta_\tau=\frac{Q}{(\rho_m C_p)u_\tau}, \tag{6}$$

where $Q=-k\frac{\partial\Theta}{\partial y}\Big|_w$ is the heat flux at the wall, u_τ is the fluid flow friction velocity, ρ_m is the mass density, and C_p is the heat capacity. The molecular thermal conductivity, k, and molecular thermal diffusivity, α, are related by $\alpha=\frac{k}{\rho_m C_p}$. The wall Reynolds number Re_τ, which is the same as δ^+, the inner normalized channel half-width $\delta^+=\frac{u_\tau}{\nu}\delta$, will play an important role in the following analysis.

The prescribed heat flux at $y = 0$ results in the boundary condition

$$\frac{Q}{\rho_m C_p} = -\alpha \frac{\partial \Theta}{\partial y}. \tag{7}$$

2.2 The fully developed state

In connection with heat transfer governed by (5) with constant heat flux Q prescribed at the wall $y = 0$ for $x > 0$, the fully developed state is approached at positions sufficiently downstream. This state is characterized by the x-derivative of the temperature being a positive constant, independent of both x and position in the channel. The value of the constant can be determined by applying energy balance to a section of the channel. It is of course proportional to Q and depends on the other physical parameters. It turns out to be $\frac{u_\tau \theta_\tau}{\delta U_B}$. In thermally fully developed flow, the temperature is a linearly increasing function of x (therefore unbounded), the rate of increase again being the above constant independent of location.

The temperature and turbulent heat flux profiles under fully developed conditions will be our primary concern. According to the definition given, in the thermally fully developed condition,

$$\frac{\partial \Theta}{\partial x} = \frac{\partial \Theta_w}{\partial x} = \frac{u_\tau \theta_\tau}{\delta U_B}, \tag{8}$$

for each y, where Θ_w is the temperature at the wall, and $U_B = \frac{1}{\delta}\int_0^\delta U(y)dy$ is the bulk mean velocity.

2.3 Scaling

Conventionally the velocity, length, and temperature units u_τ, $\frac{\nu}{u_\tau}$ and θ_τ (see Table 1) are used to normalize the averaged heat equation. This results in the usual inner-normalized mean velocity $U^+ = \frac{U}{u_\tau}$ and distance $y^+ = \frac{y}{\nu/u_\tau}$ from the wall.

A far more revealing alternative, however, is to use the units u_τ, δ, and $\theta_\tau \delta^+ Pr$. This choice again provides the inner velocity, but gives the outer normalized distance η and a new temperature variable Φ, which will be referred to the wall temperature Θ_w as explained now. To more accurately reflect the conditions of the fully developed state, we consider, in place of Θ, the (negative of the) difference between Θ and the corresponding wall temperature Θ_w at the same x-location. In all, the new variables (U^+, η, Φ) are defined by

$$U = u_\tau U^+, \quad y = \delta\eta = \frac{\nu\delta^+}{u_\tau}\eta, \quad \Phi = \frac{1}{\delta^+ Pr \theta_\tau}(\Theta_w - \Theta). \tag{9}$$

This locally defined temperature renders a self-preserving form for the temperature field. The fully developed condition implies no x-dependence, so our variables Φ and T (see below) will depend only on η.

The notation $T = \langle v^+ \frac{\theta}{\theta_\tau} \rangle$ will be used. Note that in this term, expressing turbulent heat transfer, temperature is scaled differently than in (9). This scaling of the turbulent term will render the heat equation a parameterless form (10) and will be the appropriate scaling for comparison with the molecular heat flux. Implementing these definitions yields

$$\frac{d^2\Phi}{d\eta^2} + \frac{dT}{d\eta} + r(\eta) = 0, \tag{10}$$

	Momentum Transfer	Heat Transfer
Molecular transfer unit	$\rho_m\nu$ (Viscosity)	$k = (\rho_m C_p)\alpha$ (Thermal conductivity)
Quantity transfered	$\tau_w = \rho_m\nu\frac{\partial U}{\partial y}\|_w$ (Momentum flux)	$Q_w = -(\rho_m C_p)\alpha\frac{\partial \Theta}{\partial y}\|_w$ (Heat flux)
Flux density	$\frac{\tau_w}{\rho_m}$	$\frac{Q_w}{(\rho_m C_p)}$
Flux velocity (temperature)	$u_\tau = \frac{\frac{\tau_w}{\rho_m}}{u_\tau} = \frac{\nu\frac{\partial U}{\partial y}\|_w}{u_\tau}$	$\theta_\tau = \frac{\frac{Q_w}{(\rho_m C_p)}}{u_\tau} = -\frac{\alpha\frac{\partial \Theta}{\partial y}\|_w}{u_\tau}$
Transfer coefficient	$c_f = \frac{\tau_w}{0.5\rho_m U_c^2} = \frac{2}{U_c^+ U_c^+}$	$c_h = \frac{Q_w}{(\rho_m C_p)U_c\Theta_c} = \frac{1}{U_c^+\Theta_c^+}$

Table 1: Comparison of the analogous terms utilized in the momentum transfer and heat transfer. Note that c_h is traditionally called the Stanton number St.

where

$$r(\eta) = \frac{U(\eta)}{U_B}.$$

The function $r(\eta)$ is $O(1)$ for all values of η except in a thin turbulent wall layer, where $\eta = O(1/\delta^+)$. This property will be important in the following. Equation (10) might be called an outer normalized equation of heat transport; it will be our basic thermal energy balance equation for the thermal transport problem.

Boundary conditions at $\eta = 0$ are

$$\Phi = 0, \ \frac{d\Phi}{d\eta} = 1, \ T = \frac{dT}{d\eta} = 0. \tag{11}$$

At the centerline $\eta = 1$,

$$T = 0, \ \ \frac{d\Phi}{d\eta} = 0. \tag{12}$$

The boundary condition $(11)_2$ is the form that (7) takes in the present units.

Note that neither the equation (10) nor the boundary conditions (11), (12) depend overtly on any parameter. However, while each of the terms in (10) is nominally $O(1)$, there is no reason to think that that is their actual magnitude, except for the last term $r(\eta)$, which is $O(1)$ except in the wall layer. Despite the absence of parameters δ^+, Pr occurring explicitly in (10), these two independent parameters are hidden there; the variables generally will depend on them, but in such a way that the DE is satisfied identically. Our task will be to try to make what is hidden explicit, through more rescaling.

2.4 Comparison of momentum transfer and scalar transfer

Since many researchers are more familar with the momentum equation, Table 1 is provided to draw analogies between quantities appearing in the momentum transfer and heat transfer analyses.

In this context, it is relevant to point out that in engineering applications the 'Reynolds analogy' is quite often used when $Pr = O(1)$. (Its deficiencies, at least for other values of Pr, will be brought out in the current paper.) Under the Reynolds analogy, the temperature profile is assumed to be the same as that of the velocity profile; in particular, $\frac{\Theta_c}{\theta_\tau} = U_c^+$. From the definitions of c_h and c_f as shown in Table 1, this requires $c_h = \frac{c_f}{2}$, which relates the key engineering parameters of the momentum and thermal boundary layers.

Layer	Location	Mean temperature
Molecular transport sublayer	$\delta^+\eta < \delta^+\eta_1 = \begin{cases} 12/Pr^{1/3} & \text{if } Pr \gg 1 \\ 30 & \text{if } Pr \sim 1 \\ 2/Pr & \text{if } Pr \ll 1 \end{cases}$	$\Phi \sim \eta$
Buffer layer		
Logarithmic layer	$\eta_1 \ll \eta \ll 1$	$\delta^+ Pr\Phi = \frac{1}{\kappa_\theta} \ln(\delta^+\eta) + \beta(Pr)$
Outer layer	$0.1 < \eta < 1$	$\delta^+ Pr(\Phi_c - \Phi) = g(\eta)$.

Table 2: Traditional layer structure of the turbulent thermal wall layer, adapted from [7].

3 Principal layer structure

3.1 Traditional picture

The thermal boundary layer for turbulent flow is traditionally divided into the four layers listed in Table 2, with the same physical reasoning as for the momentum boundary layer [3, 7]. With regard to Table 2, the following facts are noted.

(i) In addition to the Reynolds number, the thermal equations involve another parameter, Pr. As we shall see, this makes the thermal case more complicated, and the layer divisions are not as clear as for the momentum field.

(ii) There has to be a transitional region, 'buffer layer', between the molecular sublayer and the logarithmic layer if one accepts the traditional layer structure [6]. The extent of this 'thermal buffer layer' is not as clear as that of the 'momentum buffer layer'. One can say that it lies between the molecular sublayer and logarithmic layer, but with the extents of the latter layers not clearly defined, that definition provides little to build upon.

(iii) Kader provided coefficients in the logarithmic layer based mainly on fitting to the experimental data [7]: $\frac{1}{\kappa_\theta} \cong 2.12$ and $\beta(Pr) = (3.85Pr^{1/3} - 1.3)^2 + 2.12\ln(Pr)$, where κ_θ and $\beta(Pr)$ correspond to the κ and B for the log velocity profile, $U^+ = \frac{1}{\kappa}\ln(\delta^+\eta) + B$.

3.2 Revised principal layer structure

There are three terms in the mean heat equation (10), relating to molecular diffusion transport, turbulent transport, and streamwise mean advection (the former two are gradients of the respective fluxes). These terms sum to zero to reflect energy conservation. To estimate the relative magnitude of the terms, Figure 1 provides the ratio of the gradient of molecular diffusion flux to that of the turbulent transport flux:

$$\frac{\alpha \frac{d^2\Theta}{dy^2}}{-\frac{d\langle v\theta\rangle}{dy}} = \frac{\frac{d^2\Phi}{d\eta^2}}{\frac{dT}{d\eta}} \tag{13}$$

(1) $Pr < O(1)$: As shown in Figure 1(a), for low Reynolds number and low Prandtl number, the magnitude of the molecular diffusion term $\left|\frac{d^2\Phi}{d\eta^2}\right|$ is always larger than that of the turbulent term $\left|\frac{dT}{d\eta}\right|$. It is especially worth noting that the molecular heat transport is larger than the turbulent heat transport in the 'outer region' where the flow (velocity) is inertially dominated. Note also that $\frac{d\Phi}{d\eta}$ is larger than the turbulent heat flux, T, across the whole layer for low Pr (Figure 2). This situation is quite distinct from the momentum equation. For the momentum field, the diffusive and turbulent contributions to the time rate of change of momentum balance each other out to a position near the peak in the Reynolds shear stress, while the turbulent stress dominates the

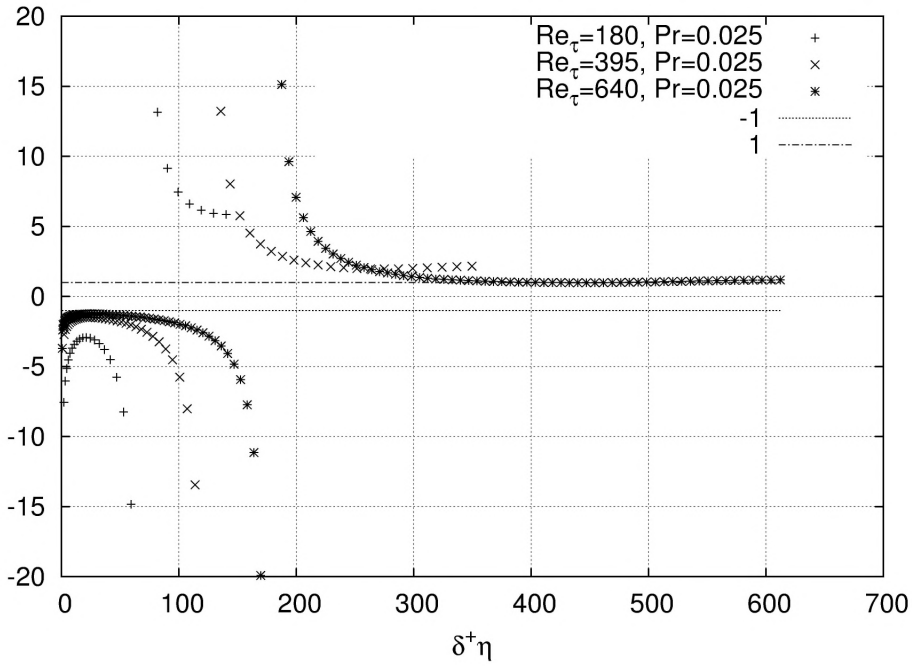

(a)

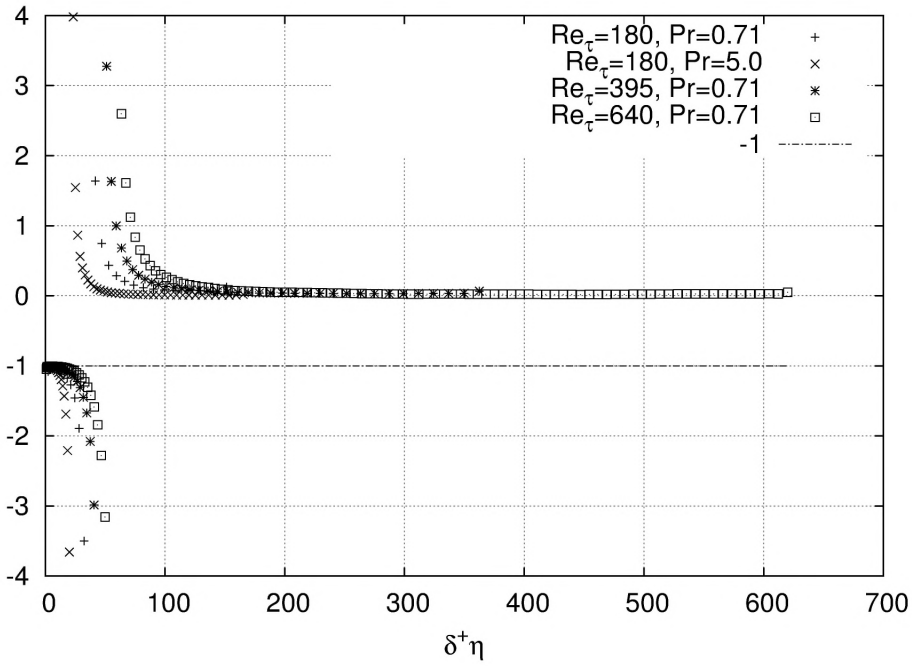

(b)

Figure 1: Heat flux gradient ratio, $\frac{\frac{d^2\Phi}{d\eta^2}}{\frac{dT}{d\eta}}$. (a) The case $Pr \ll O(1)$. (b) The case $Pr \geq O(1)$.

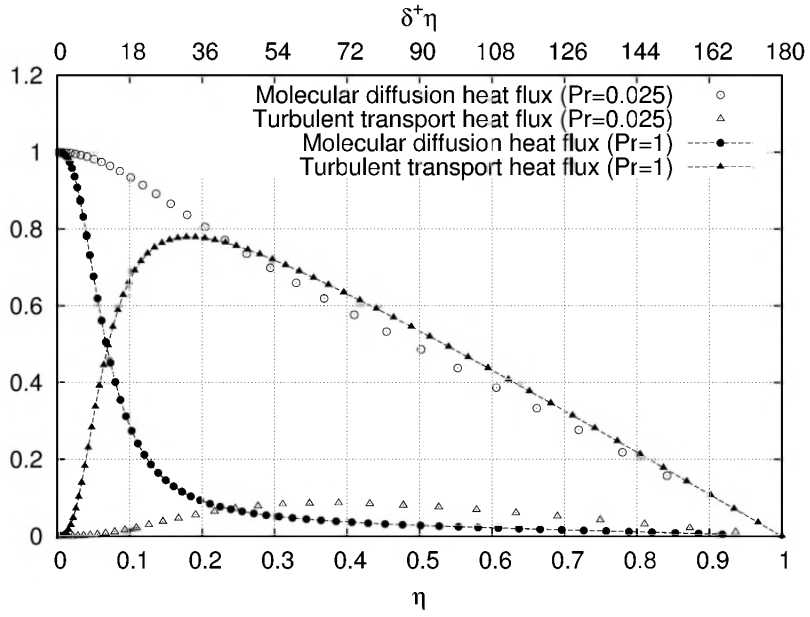

Figure 2: The molecular diffusion heat flux $\frac{d\Phi}{d\eta}$ and turbulent heat flux, $T = \langle v^+ \frac{\theta}{\theta_\tau} \rangle$ for two Prandtl numbers, in one case $Pr \ll O(1)$ and in the other, $Pr = 1$. Note that for $Pr \ll 1$ and not too high Reynolds number (i.e., $Re_\tau = 180$), $\frac{d\Phi}{d\eta}$ is always larger than T.

viscous stress beyond the buffer layer. Therefore, for low Prandtl number, the Reynolds analogy is unacceptable due to the different behavior of the terms in the equations. However even for low Pr, as Reynolds number increases (see Figure 1(a), the case when $Re_\tau = 640$ and $Pr = 0.025$), the ratio (13) approaches to -1 in a certain region near the surface.

(2) $Pr \geq O(1)$: As shown in (b) of Figure 1, there is a clear -1 ratio region. This -1 ratio region grows outward with increasing Reynolds number, and it moves inward with increasing Pr number. The reason will be explained later in Sec. 4.4.

The behavior of the ratio of the two heat flux gradient terms, as shown in Figure 1(a,b) indicate the following layer structure for $Pr > O(1)$:

- **Layer I**: Molecular diffusion/mean advection balance layer, where the molecular diffusion terms balance the mean advection term, while the turbulence term is not important. (Note that this sublayer is clearer for low Pr, as shown in Figure 1(a).)
- **Layer II**: Heat flux gradient balance layer where the heat equation balance is essentially between the molecular diffusion term and the turbulent transport term (aforementioned -1 ratio layer).
- **Layer III**: Meso layer where the all the three terms are important for the heat equation balance (except very close to the peak value of T, where the turbulent flux gradient crosses through zero and is negligible).
- **Layer IV**: Inertial layer where the heat equation balance is between the mean advection and the turbulent transport term, while the moleculear diffusion term is negligible.

UU IR Author Manuscript

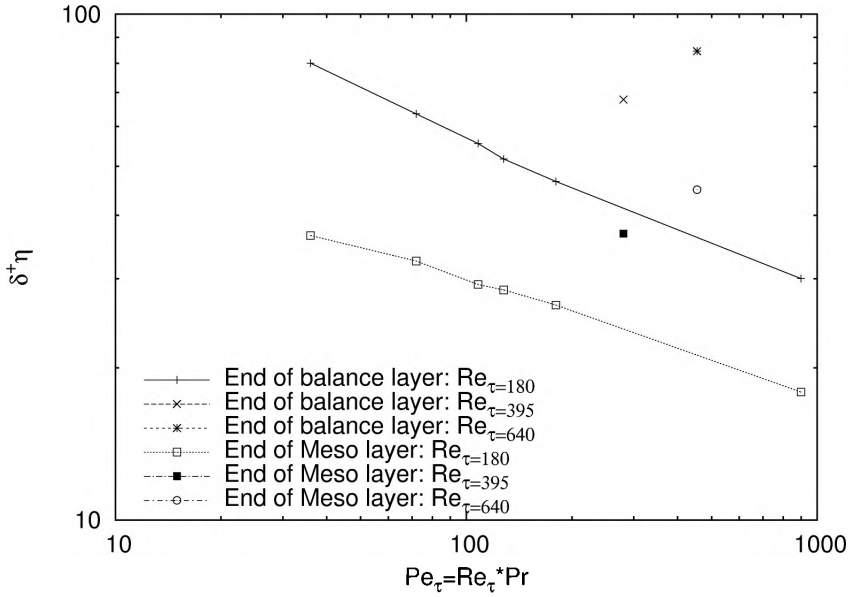

Figure 3: The inner normalized extent of the layers in fully developed thermal channel flow. It is plotted as $\delta^+\eta$ and $Pe_\tau = Re_\tau * Pr$.

3.3 Layer extents

The physical extents of the thermal layer structure shown in Fig. 3 are defined in a way similar to that for the momentum layer structures [12], i.e., the end of the gradient balance layer is defined as $(\alpha\frac{d^2\Theta}{dy^2})/(-\frac{d\langle v\theta\rangle}{dy}) = -2$, and the end of the meso layer is defined as $(\alpha\frac{d^2\Theta}{dy^2})/(-\frac{d\langle v\theta\rangle}{dy}) = 0.5$. The plots are based on the DNS data of Kawamura's group[1] [19] and Kasagi's group[2] [20]. Due to the narrow range of the Reynolds number ($Re_\tau = \delta^+ = 180, 395, 640$), and the range of Pr number ($0.025 < Pr < 5$), these data cannot reliably reveal asympototic behaviors. In Figure 3, the extent is in inner normalized distance $\delta^+\eta$, and it is plotted against $Pe_\tau = Re_\tau * Pr$. The data is for fixed Reynolds number, so Figure 3 shows that as Pr increases (or Pe_τ increases in this case), layer II and layer III move towards the wall. Note that the two Reynolds number curves are distinct under this normalization.

4 Multiscale analysis

4.1 Goals, strategies, and observations

The object now is to apply a multiscale analysis to partially explain and make a major extension of the results described in Sec. 3.

Procedure The strategy will be as follows. We begin with the scaled form (10)–(12) of the averaged energy balance differential equation and boundary conditions, in which all three terms of the DE have nominal order $O(1)$; in fact such that neither the DE nor BC have any explicit parameter dependence. The three terms, as in (5), represent the gradients of heat flux due to

[1] http://murasun.me.noda.tus.ac.jp/db/dns
[2] http://www.thtlab.t.u-tokyo.ac.jp/DNS/

(a) molecular diffusion and (b) turbulence; as well as (c) convective heat transfer by the given underlying fluid flow. The applicable Reynolds averaged DE (10) is similar in form to that which occurs in the study of steady turbulent flow in a channel. In fact, many of the tools used in the latter analysis find application in the former as well. However, the thermal problem has one extra parameter, Pr, in addition to δ^+, and this, it turns out, makes for an additional degree of indeterminacy and difficulty.

Recognizing that the nominal order of a term does not necessarily correspond to its actual order of magnitude, we next undertake to rescale the variables so that after terms of nominal order $\ll O(1)$ in the resulting DE and BC are discarded, the nominal order of each term in some part of the channel (i.e., some scaling patch or layer) coincides with its actual order of magnitude. Because of the underdetermined nature of the problem, this may involve some examination of empirical data concerning the actual magnitudes of terms.

Data indicate that with the possible exclusion of a thin wall layer, the ratio of the molecular diffusive to the turbulent heat flux gradients (ratio of term (a) to (b), referenced above) depends strongly on Pr, even though that parameter is not explicit in the energy balance equation (10). The analysis is based on this property (see the main hypothesis below), and in fact on the supposition that the ratio is very large when $Pr \ll 1$, and except in a wall layer, is very small when $Pr \gg 1$.

Using this approach, we construct scaling patches and surmise the qualitative structure of the temperature and turbulent thermal flux profiles.

4.2 Dependence of Φ and T on Pr.

Before making any hypothesis, it is useful to examine the properties of Φ with DNS data. The Reynolds number and Prandtl number dependence of Φ are shown in Figures 4. The dependences of T on those two numbers are shown in Figures 5. The centerline values Φ_c of Φ for different Prandtl numbers are shown in Figure 6(a). All of these data show a general monotone decrease of Φ as Pr increases, $\delta^+ = Re_\tau$ being held constant. This same trend, for the respective η-derivatives, can be seen in Fig. 2. In the case of the second derivatives, if one restricts attention to the outer region in Layer IV, the plots in Fig. 1 serve, to some extent, to indicate the same monotone trend, because the numerator of the ratio plotted there is just the second derivative in question, while the denominator is almost constant. The data in Fig. 6 suggest that $\Phi_c \to 0$ as $Pr \to \infty$, and that Φ_c approaches an $O(1)$ limit as $Pr \to 0$.

It is interesting to observe the dependence of the centerline value of the ratio plotted in Fig. 1 on Pr and Re_τ. Part (a) shows that it decreases with increasing Re_τ, and that this decrease is marked when Pr is as small as 0.025. Part (b) shows that when $Pr = O(1)$, the ratio is very small, independently of Re_τ.

These observations on Prandtl number dependence will be the basis for our main hypothesis below.

The monotone dependence of Φ and its derivatives upon Pr suggests that when Pr decreases, δ^+ remaining fixed, the second term in (10), $\frac{dT}{d\eta}$, decreases and the first term, $\frac{d^2\Phi}{d\eta^2}$, increases. Of course since the third term in (10) is always $O(1)$ (both nominally and actually), smallness of either of the first two terms implies that the other is $O(1)$. In view of all this, our hypothesis is

Main hypothesis *For fixed values of δ^+ and η, Φ is a monotonic decreasing function of Pr, approaching 0 as $Pr \to \infty$ and approaching an $O(1)$ limit as $Pr \to 0$. The same is true of $\frac{d\Phi}{d\eta}$ and $\left|\frac{d^2\Phi}{d\eta^2}\right|$, except that the first limit, namely as $Pr \to \infty$, is only valid outside a narrow wall layer near $\eta = 0$.*

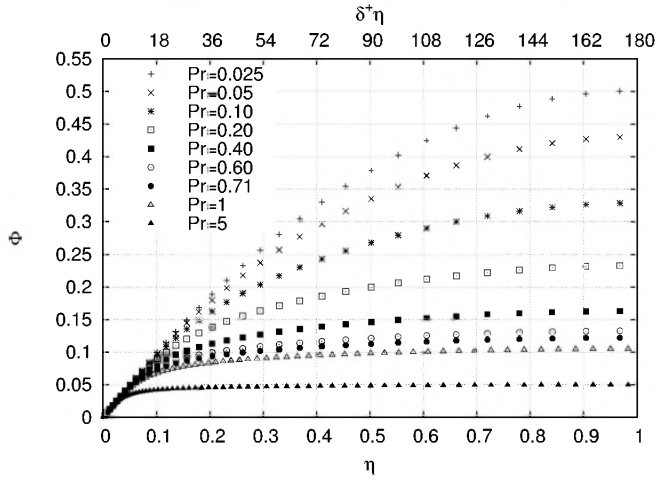

(a)

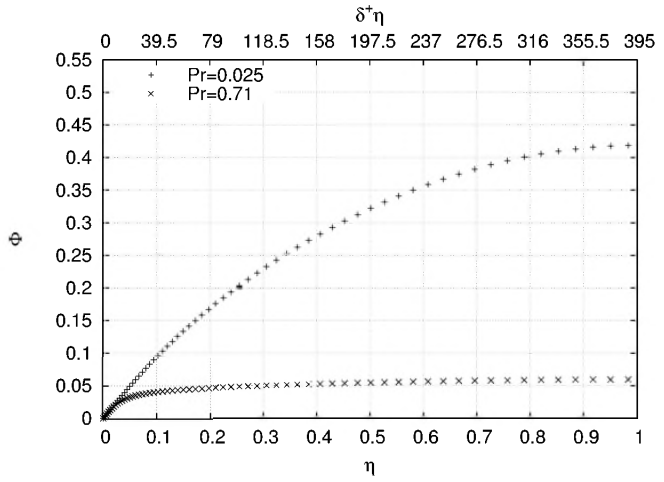

(b)

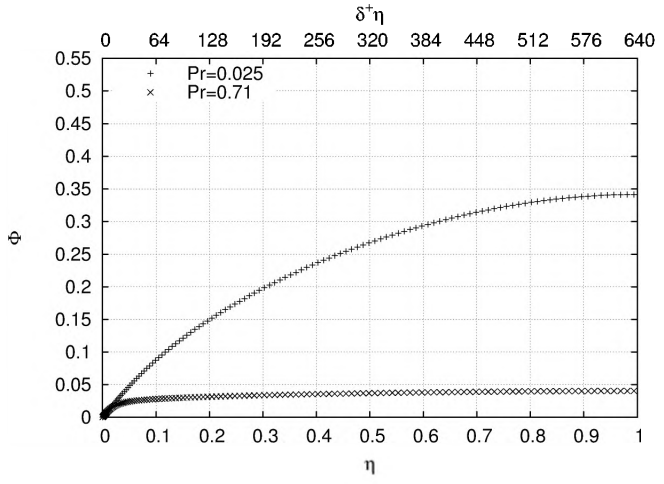

(c)

Figure 4: The Φ profiles across the half channel for different Reynolds numbers and different Prandtl numbers. (a) Fixed Reynolds number of $Re_\tau = 180$. (b) $Re_\tau = 395$. (c) $Re_\tau = 640$. The DNS data are from Kawamura's group.

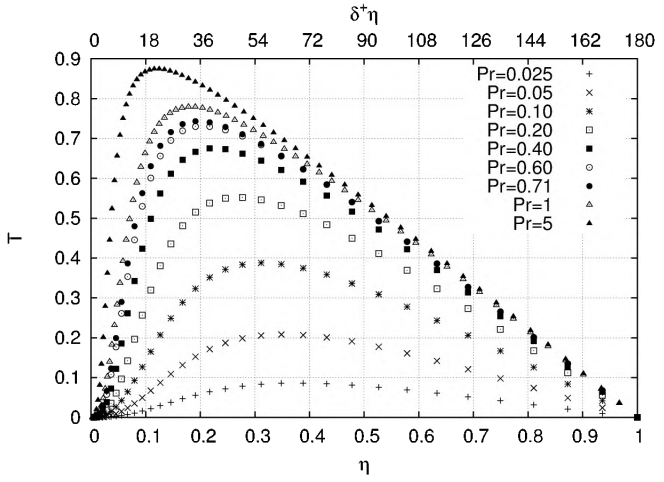

(a)

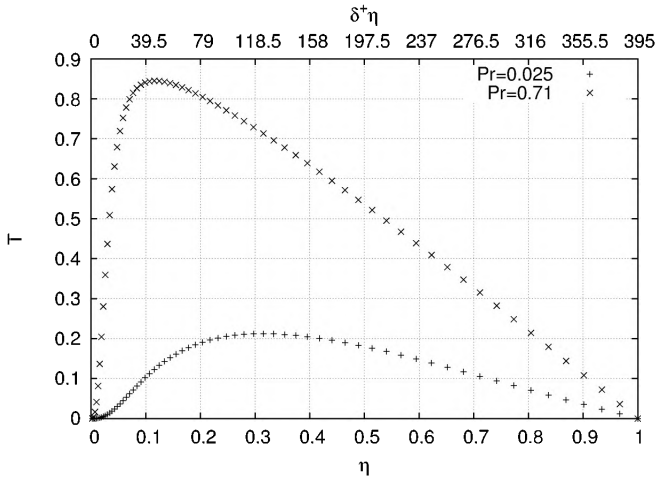

(b)

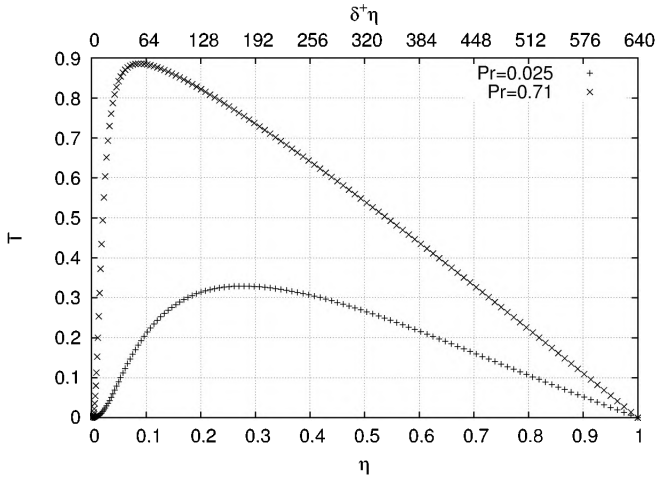

(c)

Figure 5: Turbulent heat flux, T, profiles across the half channel for different Reynolds numbers and different Prandtl numbers. (a) Fixed Reynolds number of $Re_\tau = 180$. (b) $Re_\tau = 395$. (c) $Re_\tau = 640$. The DNS data are from Kawamura's group.

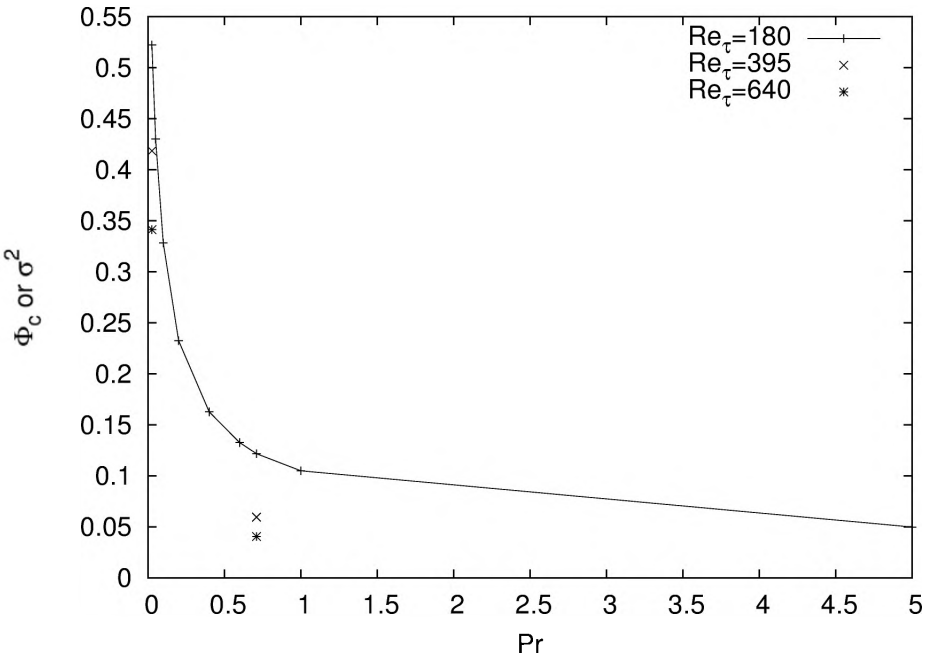

(a)

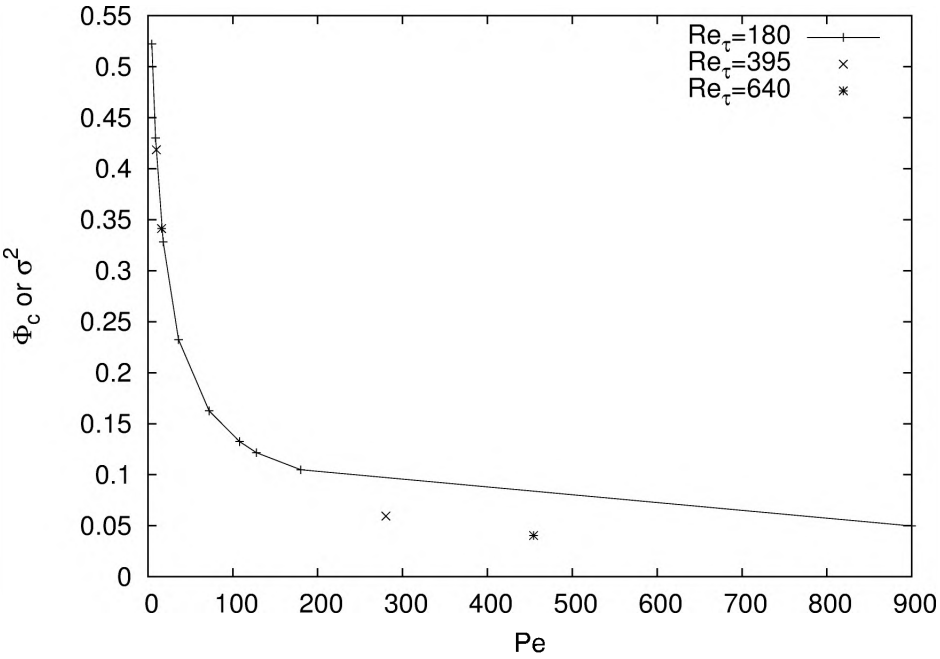

(b)

Figure 6: The dependence of centerline Φ values, Φ_c, on Prandtl number and Peclet number $Pe = Re_\tau Pr$. (a) Φ_c versus Pr. (b) Φ_c versus Pe. The DNS data are from Kawamura's group. The Reynolds number of the data are $Re_\tau = 180,\ 395,\ 640$. The Prandtl numbers are between $Pr = 0.025$ and $Pr = 5$. Note that σ^2, defined above (18) and occurring on the vertical axes, will be one of the principal parameters of the analysis to follow.

Immediate consequences of the main hypothesis are these:

(a) For each fixed large δ^+, when Pr is small enough, the second term in (10) can be neglected, resulting in a well-determined boundary value problem

$$\frac{d^2\Phi}{d\eta^2} + r(\eta) = 0, \tag{14}$$

$$\Phi(0) = 0, \ \frac{d\Phi}{d\eta}(0) = 1, \ \frac{d\Phi}{d\eta}(1) = 0, \tag{15}$$

whose unique solution can be written down, since $\int_0^1 r(\eta)\, d\eta = 1$: $\Phi(\eta) = \eta + \int_0^\eta (s-\eta) r(s)\, ds$.

(b) For each fixed large δ^+, when Pr is large enough, the first term in (10) can be neglected, except in a narrow wall layer near $\eta = 0$. Outside the wall layer, there results the approximate DE

$$\frac{dT}{d\eta} + r(\eta) = 0, \tag{16}$$

$$T(1) = 0, \tag{17}$$

which again has a unique solution.

The existence of an excluded wall layer in case (b) is necessary in order to allow the boundary conditions (11) at the wall to be satisfied. Rescalings in that layer will be necessary to bring out the structure of Φ and T there.

Remarks Under this hypothesis, when Pr is small enough, we have approximate knowledge of the variables Φ and T throughout the channel. Moreover, this is done with a single scaling: the one that produced (10). There is no other scaling needed for different ranges of the variable η. Hence there is only one "scaling patch" [13] , and it covers the entire domain.

This is not true when $Pr \gg 1$, i.e., the case in which there exists a distinct wall layer. This case entails looking for the proper rescaling(s) in that layer. These scalings will depend on Pr as well as on δ^+, both of them large parameters.

The case $Pr \ll 1$ shows a dramatic failure of the Reynolds hypothesis. The solution has $\Phi = O(1)$, which implies that the analogous inner scaled temperature difference $\Theta_w^+ - \Theta^+ = O(\delta^+ Pr)$, which may be very large. The analog in turbulent channel flow is the mean velocity U^+, which never becomes larger than $\sim C \ln \delta^+$.

The role of the Peclet number The main hypothesis was framed by choosing δ^+ and Pr as the two basic independent parameters, freezing δ^+, and letting Pr approach 0 or ∞. It may well be argued that δ^+ and the Peclet number $Pe = Pr\delta^+$ are a better choice for the basic parameters, and that we should consider what happens when δ^+ is fixed and Pe is large enough or small enough. However, a comparison of Figs. 6(a) and (b) shows little qualitative difference in the two approaches, when one considers the dependence of the centerline (maximal) value of Φ on Pr or Pe.

4.3 A paradigm

Our main unanswered question concerns the structure of the wall layer, especially its dependence on Pr. The approach here will be to build on what we know about the channel flow problem, specifically the framework established in [14, 13]. The main hypothesis will also be a crucial ingredient.

We do not consider case (a), i.e. (14), (15) when $Pr \ll 1$, because the mean temperature field has no wall layer. The initial focus is on the case when the first term in (10) is small, at least in the outer region.

Let $\sigma^2(\delta^+, Pr) = \max \Phi(\eta) = \Phi(1)$, and assume $\sigma \ll 1$. Other choices for a measure of the magnitude of Φ would serve as well for the definition of σ^2. We define the σ-dependent temperature variable Ψ by

$$\Phi = \sigma^2 \Psi, \tag{18}$$

so that $\Psi = O(1)$ near the center. With this, there exists a new outer equation

$$\sigma^2 \frac{d^2\Psi}{d\eta^2} + \frac{dT}{d\eta} + r(\eta) = 0. \tag{19}$$

We follow the lead of the inner–outer reasoning for turbulent channel flow, in which the small parameter σ is replaced by $\epsilon = (\delta^+)^{-1/2} \ll 1$, and define a new inner variable by

$$y_\sigma = \frac{\eta}{\sigma^2} \tag{20}$$

Also define a scaled advection function $r_\sigma(y_\sigma)$ by $r_\sigma(y_\sigma) = r(\eta(y_\sigma)) = r(\sigma^2 y_\sigma)$.

We obtain the following inner form for the energy balance equation:

$$\frac{d^2\Psi}{dy_\sigma^2} + \frac{dT}{dy_\sigma} + \sigma^2 r_\sigma(y_\sigma) = 0, \tag{21}$$

with boundary conditions $\Psi = T = 0$ at $y_\sigma = 0$, and (from (18), (20), and (15))

$$\frac{d\Psi}{dy_\sigma}(0) = \sigma^{-2} \frac{d\Phi}{dy_\sigma}(0) = \frac{d\Phi}{d\eta}(0) = 1. \tag{22}$$

4.4 The mesoscale and peak location

So far, the formalism is like that for the turbulent channel flow problem [12, 14], with σ replacing the parameter ϵ. It would be desirable to quantify what the present formalism predicts regarding how σ depends on δ^+ and Pr but our only source for this is DNS data (Fig. 6).

We have a σ-dependent inner variable y_σ and an outer variable η. As in [12], there will be a meso-scaled variable, valid near the maximum of T, defined by

$$\tilde{y}_\sigma = \sqrt{y_\sigma \eta} = \frac{\eta}{\sigma}. \tag{23}$$

In analogy to the channel turbulence problem, the location of this maximum is at

$$y_\sigma = y_{\sigma m} = O(\sigma^{-1}), \ \eta = \eta_m = O(\sigma) \tag{24}$$

(these relations are equivalent to each other).

Figure 7 clearly corroborates these estimates. In fact, it indicates that η_m is almost a linear function of σ, for at least the value $Re_\tau = 180$. The peak location values for the other values of Re_τ are not far away. It is expected that any approximate linear relation would have Re_τ-dependent coefficients. Given that the location of the peak value of T, measured in the outer variable η, is an increasing function of σ, the main hypothesis in turn suggests that σ, a measure of the magnitude of Φ, increases when Pr decreases (at least for $Pr \gg 1$), so that in all, the peak position, measured in η, may be expected to be a decreasing function of Pr. This is strikingly confirmed by DNS simulation results in Fig. 5.

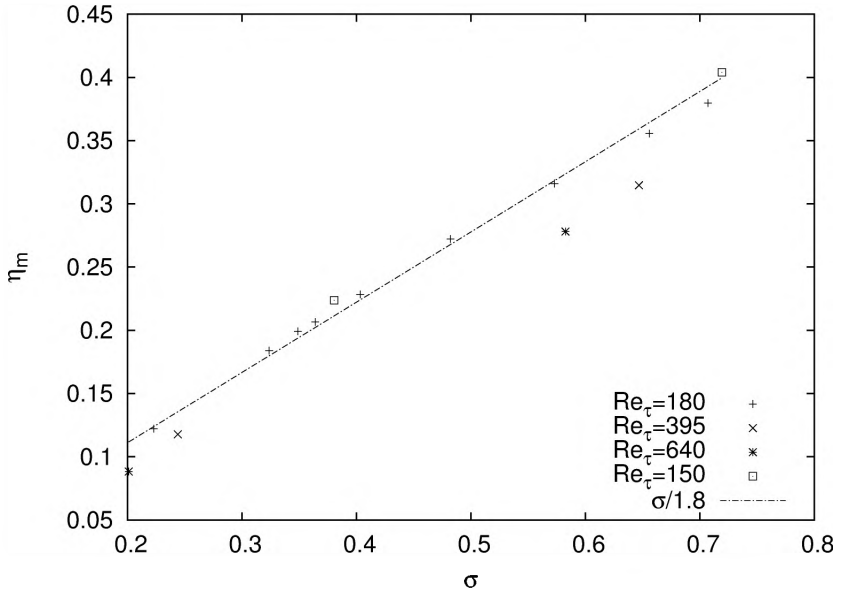

Figure 7: Maximum T location. Note that the range of $\sigma = (\frac{1}{Pr\delta^+}\frac{\Theta_w - \Theta_c}{\theta_\tau})^{0.5}$ is rather limited due to the range of the DNS data.

5 A hierarchy of layers when $Pr \gg 1$

The three scalings mentioned so far, namely inner, outer, and meso, constitute those for the primary layer structure, but there is much more structure to be found. As typified in [14, 13], the argument leading to a mesolayer at the maximum (peak) value of T can be generalized to show the existence of a whole continuum of layers, one at the peak value of each of a family of adjusted Reynolds stresses. The same can be done in the present case, since the problem formulation (19), (22) is completely analogous to that case of turbulent channel flow. The differences are now that (i) the small parameter is σ, whereas in the former case it was ϵ, which had a different physical meaning; and (ii) the convection term $r(\eta)$ is not the constant 1 (although it deviates significantly from 1 only for small η).

In this section, the procedure for showing this continuum of scales will be explained briefly; especially relevant will be the way of handling the nonconstancy of r.

5.1 The adjusted turbulent thermal fluxes

We proceed from (21), assuming that σ is so small that the graph of $T(\eta)$ has a prominent peak. To dwell somewhat on this issue, the outer approximation is obtained from (16), (17): $T(\eta) = T_{out}(\eta) \equiv \int_\eta^1 r(s)\,ds$. ¿From the outer approximation we find that the function T behaves qualitatively like the fluid's Reynolds stress: it rises to achieve a maximum near $T_{out}(0) = 1$ ($1 - T_{max} = O(\sigma)$) at a point near the wall satisfying (24), then diminishes steadily to vanish at the centerline.

To obtain the scale hierarchy, define a family of adjusted turbulent thermal fluxes:

$$T^\rho(y_\sigma) \equiv T(y_\sigma) + \sigma^2 \int_0^{y_\sigma} r_\sigma(s)\,ds - \rho y_\sigma. \tag{25}$$

Inserting this into (21) yields

$$\frac{d^2\Psi}{dy_\sigma^2} + \frac{dT^\rho}{dy_\sigma} + \rho = 0, \tag{26}$$

The next observation is that near a peak value of T^ρ, a rescaling eliminates, in (26), any explicit dependence on ρ. For a range of values of ρ, depending on σ as well as on ϵ, the function $T^\rho(y_\sigma)$ will have a strict local maximum at some point $y_\sigma = y_{\sigma m}(\rho)$, also depending on Pr and ϵ. As in the channel flow without thermal effects, the existence of a hierarchy of layers L_ρ^θ can be derived, located at $y_{\sigma m}(\rho)$, in which the intrinsic scaling is

$$dy_\sigma = \rho^{-1/2} d\hat{y}, \quad dT^\rho = \rho^{1/2} d\hat{T}, \quad T^\rho = T_m^\rho + \rho^{1/2}\hat{T}, \tag{27}$$

where $T_m^\rho = \max(T^\rho)$, leading to

$$\frac{d^2\Psi}{d\hat{y}^2} + \frac{d\hat{T}}{d\hat{y}} + 1 = 0. \tag{28}$$

Such a rescaling that yields a parameter-free differential equation, together with the satisfaction of certain conditions that ensure the compatibility of the scaling with known data in a neighborhood of $y_{\sigma m}(\rho)$, are sufficient to verify the existence of a scaling layer L_ρ^θ for each ρ in the range specified. The details are the same as those in [14, 13]. This establishes the continuum of layers, which can be combined with the inner, outer, and meso layers to provide structural information about the profiles of Φ and T.

5.2 Locations of the L_ρ^θ

To get the approximate location $y_{\sigma m}(\rho)$, the approximate profiles, note from (25) and the fact that $\frac{dT^\rho}{dy_\sigma}(y_{\sigma m}) = 0$, that

$$\frac{dT(y_{\sigma m}(\rho))}{dy_\sigma} = \rho - \sigma^2 r_\sigma(y_{\sigma m}(\rho)). \tag{29}$$

Differentiate to get

$$\frac{d^2T(y_{\sigma m}(\rho))}{dy_\sigma^2}\frac{dy_{\sigma m}}{d\rho} = 1 - \sigma^2 r_\sigma'(y_{\sigma m}(\rho))\frac{dy_{\sigma m}}{d\rho}. \tag{30}$$

Also from (27),

$$\frac{d^2T(y_{\sigma m}(\rho))}{dy_\sigma^2} = \rho^{3/2}\frac{d^2\hat{T}}{d\hat{y}^2} \equiv -A(\rho)\rho^{3/2}, \tag{31}$$

where

$$A(\rho) = -\frac{d^2\hat{T}}{d\hat{y}^2}(0) = O(1). \tag{32}$$

Thus,

$$\frac{dy_{\sigma m}(\rho)}{d\rho} = \left(-A(\rho)\rho^{3/2} + \sigma^2 r_\sigma'(y_{\sigma m}(\rho))\right)^{-1}. \tag{33}$$

In principle, if $A(\rho)$ is known, (33) can be solved for $y_{\sigma m}(\rho)$ as a function of ρ, with an integration constant C. Then the relation is inverted to get ρ as a function of $y_{\sigma m}(\rho)$ and C. Then one integrates (29) to get $T(y_\sigma)$ (with a second integration constant). Finally, integrate (21) twice to get $\Psi(y_\sigma)$ (approximately), and hence Φ from (18).

Conditions for logarithmic-like temperature profiles The easiest case is when $A(\rho)$ is constant and σ is so small that we may neglect the $O(\sigma^2)$ terms in (33), (29), and (21). In this case, straightforward calculations show that $\Phi = C_1\sigma^2 \ln(y_\sigma + C_2)$, and hence from (20) a similar logarithmic-like function of η. But when may one expect $A(\rho)$ to be constant (or almost constant)? A similarity argument, as in [14, 13] argues for the approximate constancy of $A(\rho)$ in the interior of its range in ρ, and the same argument also applies here.

Besides indicating conditions under which the temperature profile is expected to be logarithmic-like, our reasoning goes the other way: if A is not constant or the terms in σ^2 cannot reasonably be neglected, then the profile will not be logarithmic-like.

In this latter connection, it would be of interest to know when the term $\sigma^2 r'(y_{\sigma m}(\rho))$ in (33) may be neglected. For this, one might assume that r approaches its maximum at the centerline logarithmically, and r' decays like $\frac{1}{y_\sigma}$. Therefore that term might be negligible in comparison with the other term at locations y_σ where $\sigma^2(y_\sigma)^{-1} \ll \rho^{3/2}$. For example, this would be true for all $y_\sigma \gg 1$ if $\rho \geq \sigma^{4/3}$.

5.3 Scaling for T

But the goal is really to gauge the natural length scale for T in the layer L^θ_ρ, rather than T^ρ. From (25),

$$dT^\rho = dT + \sigma^2 r(y_\sigma) dy_\sigma - \rho dy_\sigma, \tag{34}$$

and from (27),

$$\rho^{1/2} d\hat{T} = dT + \sigma^2 r(y_\sigma)\rho^{-1/2} d\hat{y} - \rho^{1/2} d\hat{y}, \tag{35}$$

so that

$$dT = \rho^{1/2}\left[d\hat{T} - \left(\sigma^2 r \rho^{-1} - 1\right) d\hat{y}\right]. \tag{36}$$

Thus when L^θ_ρ is traversed, so that $\hat{y}$ and $\hat{T}$ change by an amount $\leq O(1)$, provided that the layer is located at a position y where $\sigma^2 r(y_\sigma)\rho^{-1} - 1 \leq O(1)$, then T changes by an amount $O(\rho^{1/2})$, the same as does T^ρ. In short, in L^θ_ρ, if $\rho \geq O(\sigma^2 r(y_\sigma))$, then the natural scaling for y_σ and T is still given by (27) with appropriate symbol changes.

It seems that the natural scaling for r, i.e. for U^+, at the "thermal" layer L^θ_ρ, has no great effect on the scaling of Ψ and T, which only depends rather weakly on the magnitude of r, not on its natural scaling.

6 Discussion

Fully developed thermal transport through a wall-bounded turbulent flow with constant heat flux supplied at the wall was approached via scaling considerations in coordination with observations based on DNS data. They provide a qualitative picture of the temperature and turbulent heat transfer profiles which is remarkably complete, considering that the point of departure is the averaged, therefore underdetermined, version of the thermal energy balance equation.

Although the thermal problem has many features formally in common with the classical fluid dynamical problem of steady turbulent flow through a channel, its additional independent parameter Pr brings an extra degree of uncertainty. Nevertheless, a clear qualitative picture emerges when one takes into account certain clear monotonic dependences on the parameter Pr, as seen in DNS data. In particular, the existence of a continuum of layers, a hallmark of classical turbulent flow through a channel, is also seen here for large Prandtl numbers. As a result, the existence, or

nonexistence, of logarithmic-type profiles is clarified. Among other things, the monotone variation of the peak in Reynolds thermal transport with Pr, known empirically, is predictable in the present framework.

A theme running through the present analysis is that considerable prior reasoning and certain conclusions regarding the analogous pure fluid dynamical problem can be taken over and used, with some modifications, in the present context. In doing so, the principal small parameter $\epsilon = (\delta^+)^{-1/2}$ in the former problem is replaced by the parameter σ in the latter, representing the (square root of the) deviation of the scaled centerline temperature from the wall temperature, as it depends on Pr. This latter temperature scaling is given by (9) and is not the traditional one.

Acknowledgments

This work was supported by the U. S. Department of Energy through the *Center for the Simulation of Accidental Fires and Explosions* under grant W-7405-ENG-48, the National Science Foundation under grant CTS-0120061 (grant monitor, M. Plesniak), and the Office of Naval Research under grant N00014-00-1-0753 (grant monitor, R. Joslin).

References

[1] F. P. Incropera and D. P. DeWitt. *Introduction to heat transfer.* John Wiley & Sons, first edition, 1985.

[2] W. M. Kays and M. Crawford. *Convective heat and mass transfer.* McGraw-Hill Education, third edition, 1993.

[3] B. A. Kader and A. M. Yaglom. Heat and mass transfer laws for fully turbulent wall flows. *Int. J. Heat Mass Transfer*, 15:2329–2351, 1972.

[4] Z. Warhaft. Passive scalar in turbulent flow. *Annual Review of Fluid Mechanics*, 32:203–240, 2000.

[5] P. Bradshaw and G. P. Huang. The law of the wall in turbulent flow. *Proceedings of the Royal Society of London A*, 451:165–188, 1995.

[6] A. S. Monin and A. M. Yaglom. *Statistical Fluid Mechanics.* MIT Press, Cambridge, Massachusetts, first edition, 1971.

[7] B. A. Kader. Temperature and concentration profiles in fully turbulent boundary layers. *Int. J. Heat Mass Transfer*, 24:1541–1544, 1981.

[8] A. M. Yaglom. Similarity laws for constant-pressure and pressure-gradient turbulent wall flows. *Annual Review of Fluid Mechanics*, 11:505–540, 1979.

[9] S. W. Churchill and C. Chan. Theoretically based correlating equations for the local characteristics of fully developed flow in round tubes and between parallel plates. *Ind. Eng. Chem. Res.*, 34:1332–1341, 1995.

[10] S. W. Churchill. New simplified models and formulations for turbulent flow and convection. *AIChE J.*, 42:1125–1140, 1997.

[11] S. W. Churchill. Turbulent flow and convection: The prediction of turbulent flow and convection in a round tube. *Advances in heat transfer*, 34:255–361, 2001.

[12] T. Wei, P. Fife, J. Klewicki, and P. McMurtry. Properties of the mean momentum balance in turbulent boundary layer, pipe and channel flows. *To appear in J. Fluid Mech.*, 2004.

[13] P. Fife, J. Klewicki, P. McMurtry, and T. Wei. Multiscaling in the presence of indeterminacy: wall-induced turbulence. *Under review for SIAM J. Multiscale Modeling and Simulation*, 2004.

[14] P. Fife, T. Wei, J. Klewicki, and P. McMurtry. Stress gradient balance layers and scale hierarchies in wall-bounded turbulent flows. *Under review for J. Fluid Mech.*, 2004.

[15] J. Klewicki, P. McMurtry, P. Fife, and T. Wei. A physical model of the turbulent boundary layer consonant with the structure of the mean momentum balance. In *15th Australasian Fluid Mechanics Conference*, The University of Sydney, Sydney, Australia, 2004.

[16] T. Wei, P. McMurtry, J. Klewicki, and P. Fife. Meso scaling of Reynolds shear stress in turbulent channel and pipe flows. *Under review for Phys. Fluids*, 2004.

[17] A. Perry and W. H. Schofield. Mean velocity and shear stress distributions in turbulent boundary layers. *Physics of Fluids*, 16:2068–2074, 1973.

[18] L. D. Landau and E. M. Lifshitz. *Fluid Mechanics*. Pergamon Press, London, first edition, 1959.

[19] H. Kawamura, H. Abe, and K. Shingai. DNS of turbulence and heat transport in a channel flow with different reynolds and prandtl numbers and boundary conditions. In *Turbulence, Heat and Mass Transfer 3 (Proc. of the 3rd International Symposium on Turbulence, Heat and Mass Transfer)*, pages 15–32, Aichi Shuppan, Japan, 2000.

[20] N. Kasagi, Y. Tomita, and A. Kuroda. Direct numerical simulation of the passive scalar field in a two-dimensional turbulent channel flow. In *Proc. of 3rd ASME/JSME Thermal Enginnering Joint Conference*, pages 175–182, Reno, 1991.

UU IR Author Manuscript